Appendix A Supplementary Information

A.1 Supplementary Methods

FT-IR measurements

FT-IR spectroscopy measurements were performed on both raw and cooked egg yolk and albumen in order to collect information about denaturation and aggregation of egg proteins after the cooking process. Four cooking techniques were tested, namely hard-boiling, soft-boiling, sous vide and periodic cooking. In all cases, after the egg was cooked, it was cooled down under running water and the shell was cracked open. A small amount of the sample to be tested (yolk or albumen) was then collected with a spatula and put on the instrument plate. When not liquid, a small pressure was applied on the sample to ensure sufficient adhesion to the plate.
FT-IR spectra were collected in the ATR mode using a single reflection ATR accessory (UATR from Perkin-Elmer, Newark, NJ, USA). This unit was equipped with a diamond crystal as IRE and two ZnSe crystals as transfer elements. The IRE had horizontal geometry, and an angle of incidence of 45°. The optimum wavenumber range for the present configuration was 4000–650 cm^{-1}. The ATR accessory was equipped with a pressure transducer on the crystal tip to ensure reproducible and uniform sample-to-IRE contact. Measurements were taken by a Spectrum 100 interferometer (Perkin-Elmer), equipped with a wide-band DTGS detector and a Ge on KBr beam splitter. The frequency scale was internally calibrated to 0.01 cm^{-1} using a He–Ne reference laser. 16 scans at a resolution of 4 cm^{-1} were averaged to improve the signal-to-noise ratio. Tests were performed at ambient temperature. All experiments were performed in duplicates.

Analysis of FT-IR spectra

Analysis of the FT-IR spectra was conducted with the GRAMS/AI Spectroscopy software. First, we evaluated the difference between the collected spectra with the following:

$$A_{diff} = A_s \cdot k - A_{ref} \tag{A1}$$

Where A_{diff} is the Absorbance of the difference spectrum, A_s is the Absorbance of the Sample spectrum and A_{ref} is the Absorbance of the Reference spectrum. The k coefficient was chosen so that the difference spectra resulted perfectly flat and aligned with the baseline where the two starting spectra resulted somewhat overlapped. Sample and Reference spectra were chosen as illustrated in Table A1. This operation was repeated twice, first on egg yolk and then on egg albumen.

After all Sample, Reference and Difference spectra were at hand, for both yolk and albumen, we inspected the following areas: (i) 3000 - 2800 cm^{-1} and (ii) 1850-1450 cm^{-1}. In area (i) two peaks of the lipid component can be detected, while in area (ii) the amide I region is located. As a consequence, we decided to evaluate the areas below the peaks appearing in these regions in order to obtain information about the lipid component and the protein content, respectively. Quantification of the areas (peak

Sample	Reference
Hard-boiled	Raw
Soft-boiled	Raw
6X°C	Raw
Periodic	Raw

Table A1 Legend for the evaluation of the difference spectra. Sample and Reference spectra used to perform the difference operation for both egg yolk and egg albumen.

intensities) was performed with the Integrate command on the GRAMS/AI Software, upon careful selection of the limits of integration.
After obtaining peak intensities, the following ratios were evaluated:

$$R_1 = \frac{{A_{diff}}^{(i)}}{{A_s}^{(i)}} \tag{A2}$$

$$R_2 = \frac{{A_{diff}}^{(ii)}}{{A_{ref}}^{(ii)}} \tag{A3}$$

Where ${A_{diff}}^{(i)}$ and ${A_s}^{(i)}$ are the areas below the peaks in region (i) of the Difference and Sample spectra, respectively. Similarly, ${A_{diff}}^{(ii)}$ and ${A_{ref}}^{(ii)}$ are the areas below the peaks in region (ii) of the Difference and Reference spectra, respectively.
Equation A2 was used to evaluate the lipid amount variation for each cooking technique. This equation was used only in the case of yolk because this is the only egg phase that contains lipids. On the other hand, Equation A3 was used to evaluate the protein amount variation for each cooking technique. This equation was used in the case of both egg albumen and egg yolk. In the case of albumen, this quantity corresponded with the total amount of denatured proteins in terms of β-sheets formation, because only a sharp peek at around 1620 cm^{-1}, associated with β-sheet formation, could be detected. In the case of yolk, this quantity corresponded with a more generic protein amount variation, because it wasn't always possible to detect the sharp peak at 1620 cm^{-1}. In order to be able to compare the results of protein variation in egg yolk and egg albumen, we assumed that protein denaturation in hard-boiled egg yolk/albumen was the maximum possible and all other protein denaturation levels were evaluated in proportion. In this way, a proper cooking index was defined:

$$\text{Cooking index} = \frac{R_2(s) \cdot 100}{R_2(hard - boiled)} \tag{A4}$$

Where $R_2(s)$ is the R_2 ratio evaluated for all the cooking methods and $R_2(hard - boiled)$ is the R_2 ratio evaluated in the case of hard-boiling.

Texture Profile Analysis

TPA was performed at room temperature on the 4 different egg products (Hard-boiled, Soft-boiled, Sous vide and Periodic), after proper sample preparation. Immediately

	Evaluation	Definition
Hardness	Peak force at first compression	Firmness
Cohesiveness	A_2/A_1	How well the product withstands a second deformation relative to its resistance under the first deformation
Springiness	d_2/d_1	How well a product springs back after deformation during the first compression
Chewiness (solids)	Hardness x cohesiveness x springiness	Work required to masticate the sample to be swallowed in the case of solids
Gumminess (semi-solids)	Hardness x Cohesiveness	Work required to masticate the sample to be swallowed in the case of semi-solids

Table A2 Definition of the TPA characteristics. TPA characteristics evaluated from the force-time curve obtained with the double compression test. A_1 is the total energy required for the first compression, A_2 is the total energy required for the second compression, d_1 is the distance on the x-axis between beginning and peak of first compression and d_2 is the distance on the x-axis between beginning and peak of second compression.

after cooking, each of the egg products was cooled under running fresh water and peeled. Then, the albumen and the yolk were manually separated and a cylinder of 10 mm height and 15 mm diameter was obtained from both of them with the help of a mould. Each of the cylinders was then subjected to a two cycle compression test. The machine used for the mechanical tests was a rotational rheometer (MCR 502, Anton Paar, Graz, Austria) equipped with a parallel-plate loading configuration. The compression tool used was a flat-plate of 25 mm in diameter (diameter of the plate was chosen to be bigger than diameter of the sample) and it was positioned at a distance of 15 mm from the top of the cylindrical sample at the beginning of the test. The sample was then compressed to 80% of its original height at a speed of 2 mm/s. A waiting time of 2s separated the two consecutive compressions. Multiple textural parameters were identified from the force-time curve thus obtained. These were evaluated for both yolk and albumen as the mean of 4 replicates and are shown in Table A2.

Quantitative Descriptive Analysis

Quantitative Descriptive Analysis (or Sensory Analysis) was performed thanks to the collaboration with Adacta International. The study examined the 4 different products (Hard boiled, Soft boiled, Sous vide and Periodic). All products were cooked before the start of each planned session and were then evaluated by a panel of 8 trained assessors. The assessors measured the intensity of the characteristics shown in Table A3, Table A4 and Table A5 on a 1-9 point scale. Overall, each judge evaluated each product twice. The measurements were conducted in the Sensory room designed according to ISO 8589, following the methodology indicated in UNI EN ISO 13299. The analysis was conducted in three steps: evaluation of egg albumen, yolk and whole product (albumen + yolk). For each of these steps, the average values of the perceived intensities of each characteristic were evaluated.

Attributes	Definition
Hardness to cut	Tendency of the product to resist transversal cutting with a spoon (extremely soft to extremely hard)
Overall odour	Overall intensity of orto-nasal odour (smell) of the product
Overall flavour	Overall intensity of retro-nasal odour (flavour) of the product
Easiness of swallowing	Easiness/speed of the product swallowing

Table A3 Definition of the sensory characteristics of the whole egg product. Description and definition of the sensory attributes (characteristics) used in the evaluation of the whole product (egg albumen + yolk).

Attributes	Definition
Shininess	Degree of shininess/glossiness of the albumen surface (from not at all shiny/opaque to extremely shiny/glossy)
White colour	Intensity of white colour (from extremely light/transparent to extremely dark/yellow)
Softness	Tendency of the egg albumen to yield softly to pressure between the teeth during chewing
Wetness	Intensity of perceived wetness during chewing
Meltability	Speed at which the egg albumen melts/dissolves by compressing it between tongue and palate
Sweetness	Typical fundamental taste of sucrose in egg albumen
Umami	Typical basic taste of monosodium glutamate in egg albumen
Bitterness	Fundamental taste typical of caffeine in egg albumen
Saltiness	Typical fundamental taste of sodium chloride in egg albumen
Astringency	Tactile attribute (in the mouth) indicating the intensity of the sensation of dryness and roughness of the oral mucosa
Overall flavour	Overall intensity retro-nasal odour (flavour) of egg albumen

Table A4 Definition of the sensory characteristics of egg albumen. Description and definition of the sensory attributes (characteristics) used in the evaluation of the egg albumen.

Attributes	Definition
Shininess	Degree of shininess/glossiness of the yolk surface (from not at all shiny/opaque to extremely shiny/glossy)
Orange colour	Intensity of orange colour (from extremely light/yellow to extremely dark/almost red)
Density/body	Tendency of the yolk to oppose resistance to pressure between the tongue and palate
Pastiness	Tendency of the yolk to form a dense, compact mass during chewing that is difficult to swallow
Adhesiveness	Tendency of the yolk to stick/paste to the palate and teeth during chewing
Powderiness	Intensity of the sensation of sandiness/graininess of the yolk during crushing between tongue and palate
Wetness	Intensity of perceived wetness during chewing
Solubility	Speed at which the yolk melts/dissolves by compressing it between tongue and palate
Sweetness	Typical fundamental taste of sucrose in the yolk
Umami	Typical basic taste of monosodium glutamate in the yolk
Bitterness	Fundamental taste typical of caffeine in the yolk
Saltiness	Typical fundamental taste of sodium chloride in the yolk
Astringency	Tactile attribute (in the mouth) indicating the intensity of the sensation of dryness and roughness of the oral mucosa
Overall flavour	Overall intensity retro-nasal odour (flavour) of the yolk

Table A5 Definition of the sensory characteristics of egg yolk. Description and definition of the sensory attributes (characteristics) used in the evaluation of the egg yolk.

Sampling procedure for metabolomic analysis

A total of twenty commercially available eggs were collected for metabolomic analysis. The eggs were randomly divided into the four distinct cooking groups (n=5 per group) proposed in the current work, namely: (i) hard boiled, (ii) soft boiled, (iii) sous-vide, and (iv) periodic. Following the cooking procedure, all eggs were stored at 4 °C until analysis. In particular, the albumens and yolks of three eggs from each group underwent ^{1}H-NMR based metabolomic analysis. Additionally, the yolks of the remaining two eggs from each group were subjected to MS-based analyses to determine their amino acid and polyphenol content.

^{1}H-NMR-based analysis

Eggshells were removed from a total of twelve eggs (n=3 per group). Subsequently, yolks and albumens were meticulously separated and metabolome extraction was performed according to two different protocols.
The entire yolks were placed in 50 mL plastic tubes and stored in a freezer at −80 °C. All frozen yolks were then freeze-dried for 48 hours. Next, 450 mg of the freeze-dried powder was collected in a 50 mL plastic tube, followed by the addition of 5.626 mL of methanol and 2.810 mL of chloroform. All samples were vigorously vortexed for 30 seconds at 15-minute intervals (4 cycles). Then, 8.550 mL of chloroform and 2 mL of a 0.2 M aqueous solution of potassium chloride were added, and the samples were vortexed again for 30 seconds. Finally, the biphasic mixtures were centrifuged at 4000 rpm for 10 minutes at 4 °C, and 15 μL of the resultant upper layer (aqueous phase) were carefully transferred to Eppendorf tubes.
Additionally, 18 g of each egg albumen were manually chopped into a homogeneous mixture and collected in 50 mL plastic tubes. Then, 12 mL of methanol were added and samples underwent a cycle of vortexing for 60 seconds, followed by centrifugation (12000 rpm, 20 min, 4 °C). Subsequently, 2 mL upper supernatant were transferred in 15 mL plastic tubes, followed by the addition of 6 mL of methanol. Samples underwent another cycle of vortexing for 60 seconds and centrifugation (12000 rpm, 20 min, 4 °C). Finally, 50 μL of the resultant upper supernatant were transferred into Eppendorf tubes.
Both the albumen and yolk extracts were dried using a SpeedVac Concentrator (Thermo Fisher Scientific, Waltham, MA, USA) for 3 hours and then lyophilized overnight to remove residual solvents. The dried samples were dissolved in 220 μL of D_2O, centrifuged to remove any suspended debris (14000 rpm, 20 min, 4 °C) and 200 μL of the upper supernatant were then transferred into 3-mm NMR tubes.
One-dimensional ^{1}H-NMR spectra were recorded at 298 K using a Bruker Avance NEO 600 MHz spectrometer (Bruker Biospin GmbH, Rheinstetten, Germany) equipped with a QCI cryo-probe for 3 mm sample tubes and an autosampler (SampleJet). The spectra of hydrophilic albumen and yolk extracts were acquired by means of Topspin 4.1 (Bruker Biospin GmbH, Rheinstetten, Germany), using the 'noesygppr1d' pulse sequence to obtain the suppression of water trace signal (presaturated at 4.701 ppm). Before beginning the experiment, samples were kept at 298 K for 300 s in the probe. The acquisition parameters comprised an acquisition time of 2.62 seconds, a relaxation

delay of 4 seconds, 256 scans, 4 dummy scans, a receiver gain of 101 and a spectral width of 12,500 (20.8287 ppm). All samples underwent automatic tuning, matching, and shimming. Prior to Fourier transformation, an exponential weighting function equivalent to a 0.3-Hz line-broadening factor was multiplied by the FIDs. Then, the TopSpin built-in processing tools were used on the transformed spectra to automatically calibrate and adjust for phase and baseline distortions.
The assignment of the metabolites was realized by (i) analysis of literature data [1] and (ii) employing the peak fitting routine integrated within the evaluation edition of Chenomx NMR Suite 8.4 software (version 10.12, Chenomx Inc., Edmonton, Alberta, Canada, https://www.chenomx.com, date of last access: 5 June 2024). NMR spectra were then introduced into MATLAB (R2021a; MathWorks Inc., Massachusetts, USA), where the spectral regions without relevant signals were removed and only the region between 9 ppm and 0 ppm was kept. An interval-based alignment step was carried out using the icoshift algorithm [2] to correct for spectral misalignment and glucose doublet at 5.22 ppm was chosen as reference signal. Next, the peak areas of 17 well-separated and safely assigned metabolites found in both the albumen and yolk spectra were individually integrated, allowing to reduce the model complexity. Therefore, a data matrix made of 24 rows (samples) x 17 columns (metabolites) was submitted to a PCA [3] through the PLS toolbox version 8.6.1 (Eigenvector Research, Manson, Washington, USA) under MATLAB environment. Before the analysis, data was normalized, according to the total area (1-Norm) as well as autoscaled. Autoscaling is needed to compute PCA, in order to give to all metabolites the same chance to affect the model by employing the standard deviation as a scaling factor together with the mean-centering.

UHPLC Q-Orbitrap HRMS based analyses

A total of eight egg yolk samples (n=2 per group) were subjected to the analyses. The entire yolks were placed in 50 mL plastic tubes and stored in a freezer at −80 °C, then the frozen yolks were freeze-dried for 48 hours and stored at −20 °C.
The method used to extract polyphenolic compounds from egg yolk samples followed a previously established procedure with some modifications [4]. Freeze-dried samples (0.5 g) were extracted using 5 mL of a mixture of (MeOH:H_2O, 80:20 (v/v)). The mixture was adjusted to a pH of 1.5 by adding 1M HCl. Then the sample was subjected to an ultrasonication process for 15 min. After this step, the mixture was subjected to rotary agitation for 15 min at room temperature and next to centrifugation at 5000 rpm for 5 min at 4 °C. The resulting supernatant was collected and evaporated under vacuum at 35 °C and reconstituted with 0.5 mL of methanol. The mixture obtained was subjected to ultracentrifuge 14000 rpm for 3 min, and finally, the supernatant was recovered, diluted in methanol with 0.1% formic acid and analyzed.
The extraction of free amino acids from egg yolk was executed by following the method optimized by Carrera et al. [5].
The quali-quantitative analyses of polyphenols and amino acids were performed using a UHPLC system (Dionex UltiMate 3000; Thermo Fisher Scientific, Waltham, MA, United States) equipped with a degassing system, a quaternary UHPLC pump, and an autosampler device coupled to Q-Exactive HRMS. Chemical characterization of

polyphenols was performed by using the method previously described by Izzo et al. [6] and amino acids analyzed following the method reported by Poojary et al. [7]. Data obtained were processed using the Quan/Qual Browser Xcalibur software 3.1.66.19 (Xcalibur; Thermo Fisher Scientific, Waltham, MA, United States).
The TPC was determined through a spectrophotometric assay: Folin–Ciocalteu. TPC was measured on the diluted extract following the method reported by Izzo et al. [8]. All the experiments were conducted in triplicate. The results were expressed in mg GAE/100 g of fresh weight. Antioxidant activity was evaluated by two different spectrophotometric assays named DPPH [9] and ABTS [10] tests. All experiments were performed in triplicate. Results were expressed as mmol of Trolox/kg dry weight of sample.
Extraction of carotenoids was performed following the protocol proposed by Izzo et al. [6]. Specifically, lutein quantification was performed using the HPLC-DAD and the absorbance of lutein was measured at 450 nm.
The matrices containing the polyphenols, amino acids, TPC, DPPH, ABTS and carotenoids data were then imported in MATLAB environment to be investigated through a PCA performed with the PLS toolbox version 8.6.1 (Eigenvector Research, Manson, Washington, USA). The three data matrices were concatenated to generate an individual data matrix, made of 8 rows (samples) and 38 columns (variables). Before PCA, columns with too many missing values were deleted to not affect the model computation. Thus, the final data matrix was made of 32 columns. Also, data were pre-processed with the autoscale function.

A.2 Supplementary Discussion

Microbiological considerations

It is widely known that eggs are a dangerous vehicle for pathogen transmission, like Salmonella. Indeed, the eggshell presents a porous structure that is ideal for microorganisms to hide, and the inside of the egg, mainly the yolk, is a rich medium to support microbial growth [11]. To eliminate this hazard from the food supply, pasteurization or any other heat treatment capable of achieving a 5-log reduction (99.999%) of this pathogen must be employed [12].
Licciardiello et al. in their work [13] studied the cooking time required for shell-on eggs to reduce their salmonella population to the above mentioned insignificant level. They obtained a phantom death time curve of four types of Salmonella by plotting the log decimal reduction time as a function of the heating temperature. From this, they were able to calculate the thermal death time of the specific Salmonella species as the time required for a nine log cycle kill. We exploited these data to evaluate the survival of Salmonella, more specifically S. seftenberg 775W (that has the highest known heat resistance of any of the salmonellae [14]), in eggs cooked with the periodic cooking method. In so doing, we were able to determine that no microbiological issue arises from our novel cooking methodology. Indeed, the thermal death time after the yolk has reached the average temperature of 67°C is of 10 min, much lower than the actual cooking time at that temperature.

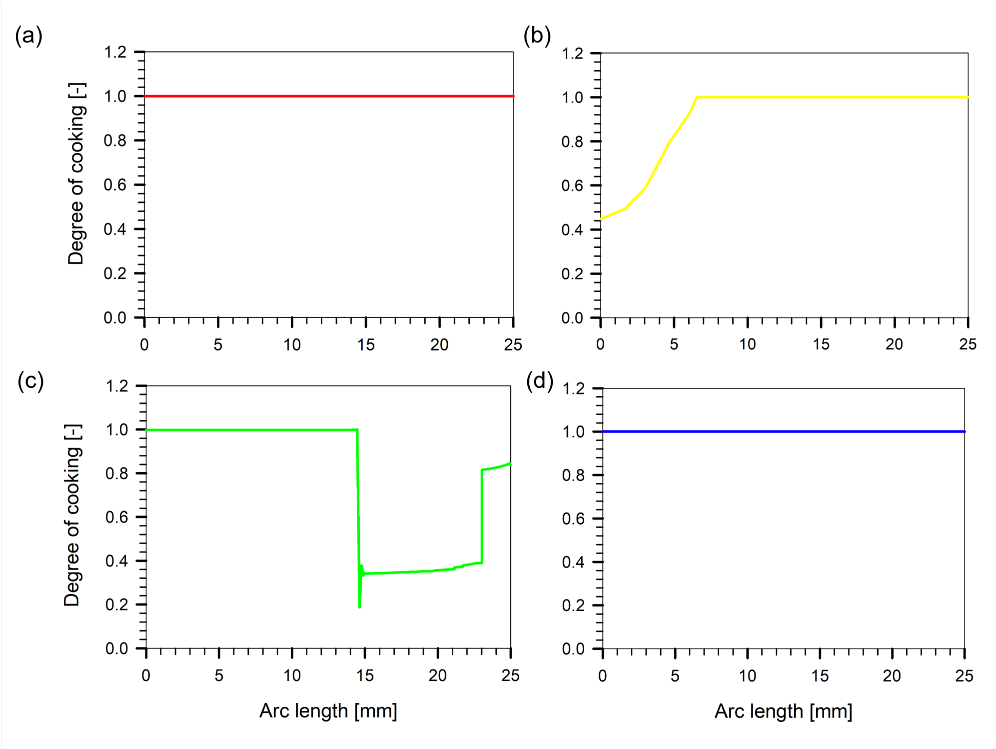

Fig. A1 Final degree of cooking of examined cooking techniques. Comparison between the final degrees of cooking of a hard-boiled (a), soft-boiled (b), sous vide (c) and periodic cooked (d) egg.

Cooking simulations

Proper comparison between all the cooking methods in terms of degree of cooking at the end of the required cooking time is shown in Figure A1.
Comparison of the cooking rates in periodic cooking and hard-boiling is also provided (Figure A2).

FT-IR spectra

IR spectra of egg albumen and yolk cooked with the different cooking techniques (hard-boiling, soft-boiling, sous vide and periodic cooking) are shown in Figure A3-A10, each one completed with a close up on the regions of interest and the corresponding difference spectrum (purple). A black dotted line is added to indicate the baseline used for protein quantification in the Amide I region, and a grey dotted line is added to indicate the baseline used for lipid quantification in the area between 3000 and 2800 cm^{-1}. Where present, the aggregation band, indicating β-sheet formation, is highlighted with a purple arrow.
It is important to note that the aggregation band is always visible in the case of egg

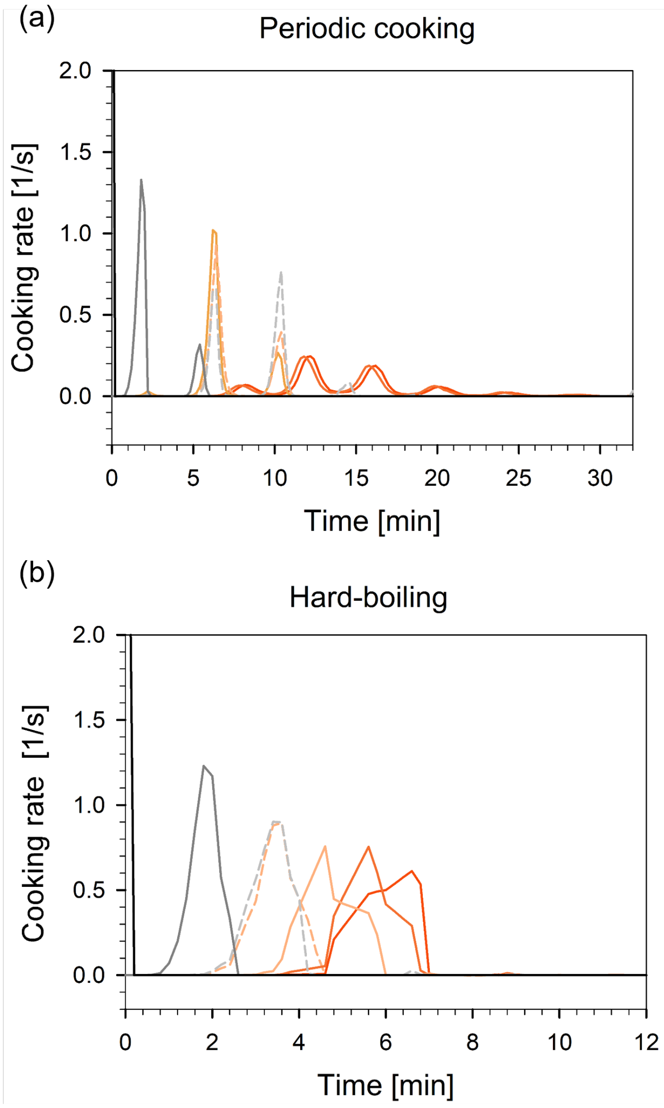

Fig. A2 Cooking rates comparison. Evolution over time of the cooking rate of an hard-boiled (a) and of a periodic-cooked egg (b).

albumen (Figures A7-A10), but not in the case of egg yolk (Figures A3-A6), where it can be clearly detected only in the case of hard-boiled egg yolk, probably due to interferences with other peaks in the area. Nonetheless, as shown by the black baseline, quantification of protein variation was always possible (Figure A4-A6).

As a final point, the lipid amount in egg yolk with the different cooking techniques was evaluated (as described in section A.1). Results are shown in Figure A11. Here, a variation in the lipid content is actually detectable at the end of the cooking processes.

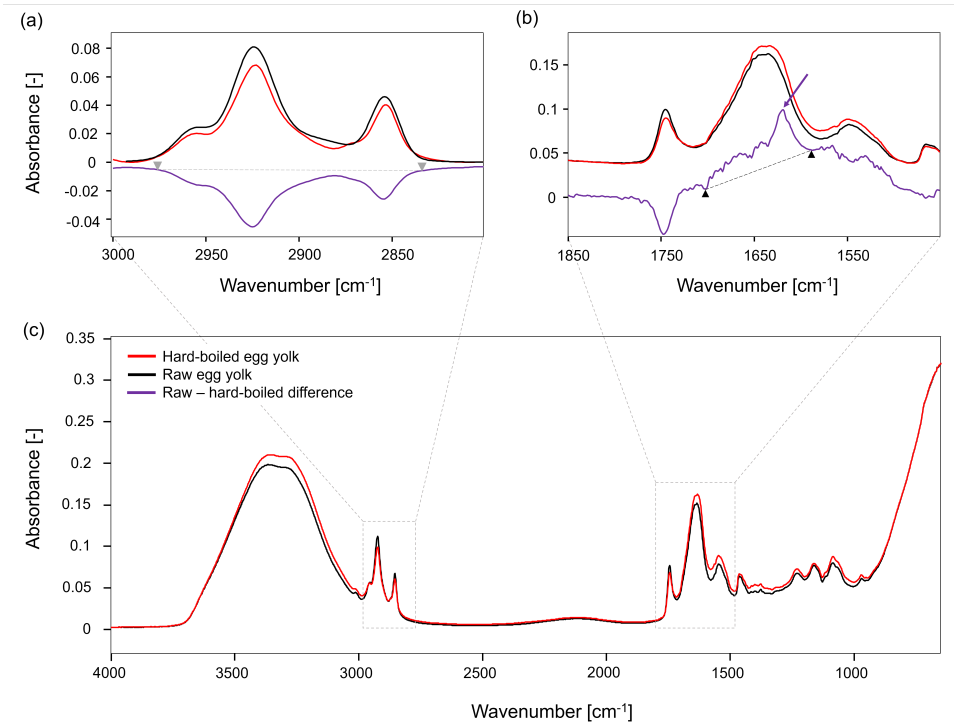

Fig. A3 IR spectra of raw and hard-boiled egg yolk. IR spectra of raw (black) and hard-boiled (red) egg yolk over the whole IR range (c); close up on band no. 2 and 3 (a) and on band no. 4 and 5 (amide I region) (b) with addition of the difference spectrum magnified x5 (purple) and the baseline used for area quantification in the Amide I region (black dotted line) and in the region between 3000 and 2800 cm^{-1} (grey dotted line). The purple arrow indicates the appearance of the aggregation band.

In particular, in the case of the hard-boiled egg yolk, the ratio decreases, which means that the lipid amount decreases with respect to its raw counterpart (also evident from the higher intensity of the water band in the hard-boiled egg yolk). The hypothesis for this behavior is that there is an exchange in nutrients between the egg albumen and the egg yolk as the cooking proceeds. Unfortunately, this behavior is not confirmed by the analysis of the other cooking techniques, so no clear trend can be found. Further exploration is needed to understand this behavior.
In the case of egg albumen, no ratio has been evaluated because no peak related to lipid component can be detected in the raw albumen spectrum. Neverthless, in all of the spectra of cooked egg albumen some peaks seem to appear at the typical lipid component frequencies, with a behavior that appears to be complementary to that seen in egg yolk. The hypothesis of the exchange in nutrients seems to be confirmed, despite the lack of a clear trend.

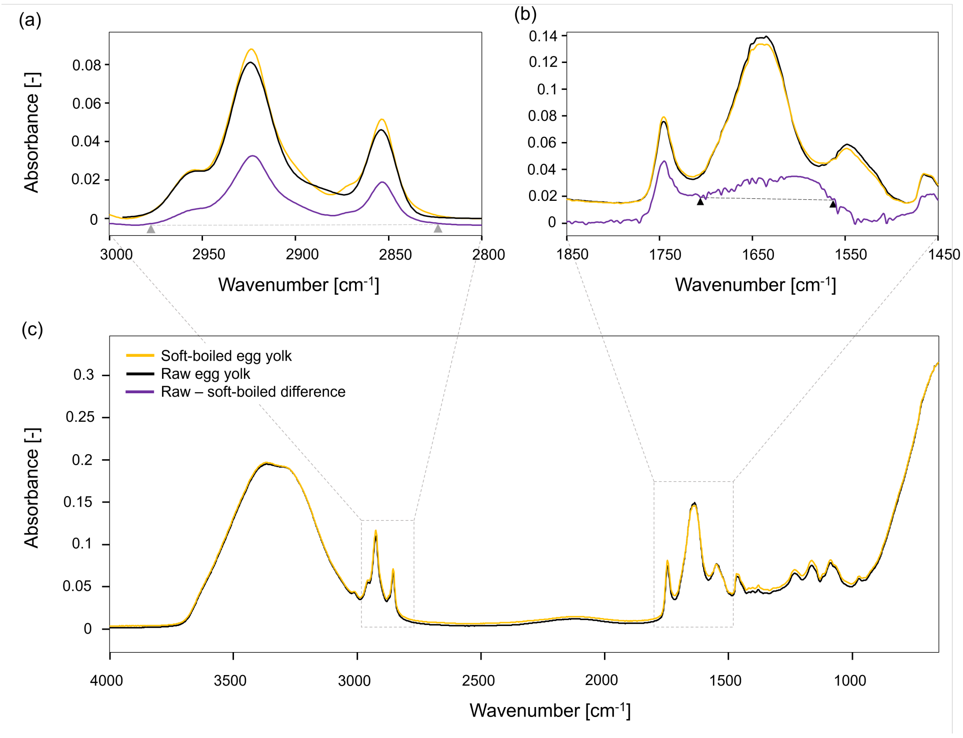

Fig. A4 IR spectra of raw and soft-boiled egg yolk. IR spectra of raw (black) and soft-boiled (orange) egg yolk over the whole IR range (c); close up on band no. 2 and 3 (a) and on band no. 4 and 5 (amide I region) (b) with addition of the difference spectrum magnified x5 (purple) and the baseline used for area quantification in the Amide I region (black dotted line) and in the region between 3000 and 2800 cm^{-1} (grey dotted line).

References

[1] Xia, F., Zhao, Y., Xing, M., Sun, Z., Huang, Y., Feng, J., Shen, G.: Discriminant analysis of the nutritional components between organic eggs and conventional eggs: a 1h nmr-based metabolomics study. Molecules **27**(9), 3008 (2022)

[2] Savorani, F., Tomasi, G., Engelsen, S.B.: icoshift: A versatile tool for the rapid alignment of 1d nmr spectra. Journal of magnetic resonance **202**(2), 190–202 (2010)

[3] Hotelling, H.: Analysis of a complex of statistical variables into principal components. Journal of educational psychology **24**(6), 417 (1933)

[4] Nimalaratne, C., Lopes-Lutz, D., Schieber, A., Wu, J.: Free aromatic amino acids in egg yolk show antioxidant properties. Food Chemistry **129**(1), 155–161 (2011)

[5] Carrera Fernández, C.A., Ruiz Rodríguez, A., Palma Lovillo, M., García Barroso, C., et al.: Ultrasound-assisted extraction of amino acids from grapes (2015)

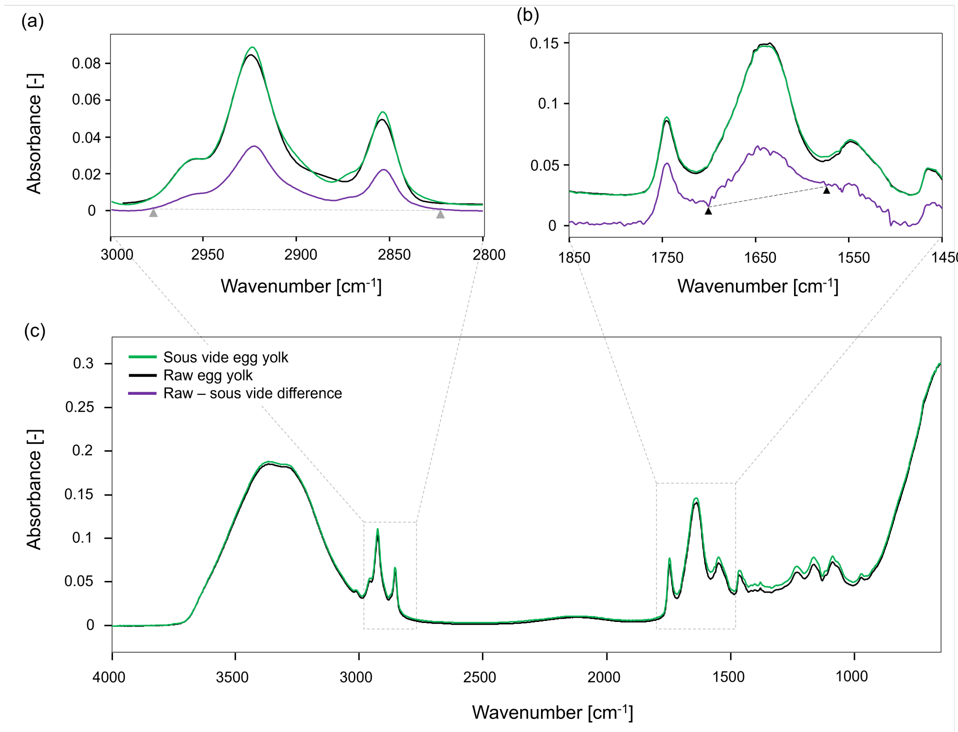

Fig. A5 IR spectra of raw and sous vide egg yolk. IR spectra of raw (black) and sous vide (green) egg yolk over the whole IR range (c); close up on band no. 2 and 3 (a) and on band no. 4 and 5 (amide I region) (b) with addition of the difference spectrum magnified x5 (purple) and the baseline used for area quantification in the Amide I region (black dotted line) and in the region between 3000 and 2800 cm^{-1} (grey dotted line).

[6] Izzo, L., Castaldo, L., Lombardi, S., Gaspari, A., Grosso, M., Ritieni, A.: Bioaccessibility and antioxidant capacity of bioactive compounds from various typologies of canned tomatoes. Frontiers in Nutrition **9**, 849163 (2022)

[7] Poojary, M.M., Tiwari, B.K., Lund, M.N.: Selective and sensitive uhplc-esi-orbitrap ms method to quantify protein oxidation markers. Talanta **234**, 122700 (2021)

[8] Izzo, L., Pacifico, S., Piccolella, S., Castaldo, L., Narváez, A., Grosso, M., Ritieni, A.: Chemical analysis of minor bioactive components and cannabidiolic acid in commercial hemp seed oil. Molecules **25**(16), 3710 (2020)

[9] Cavallo, P., Dini, I., Sepe, I., Galasso, G., Fedele, F.L., Sicari, A., Bolletti Censi, S., Gaspari, A., Ritieni, A., Lorito, M., *et al.*: An innovative olive pâté with nutraceutical properties. Antioxidants **9**(7), 581 (2020)

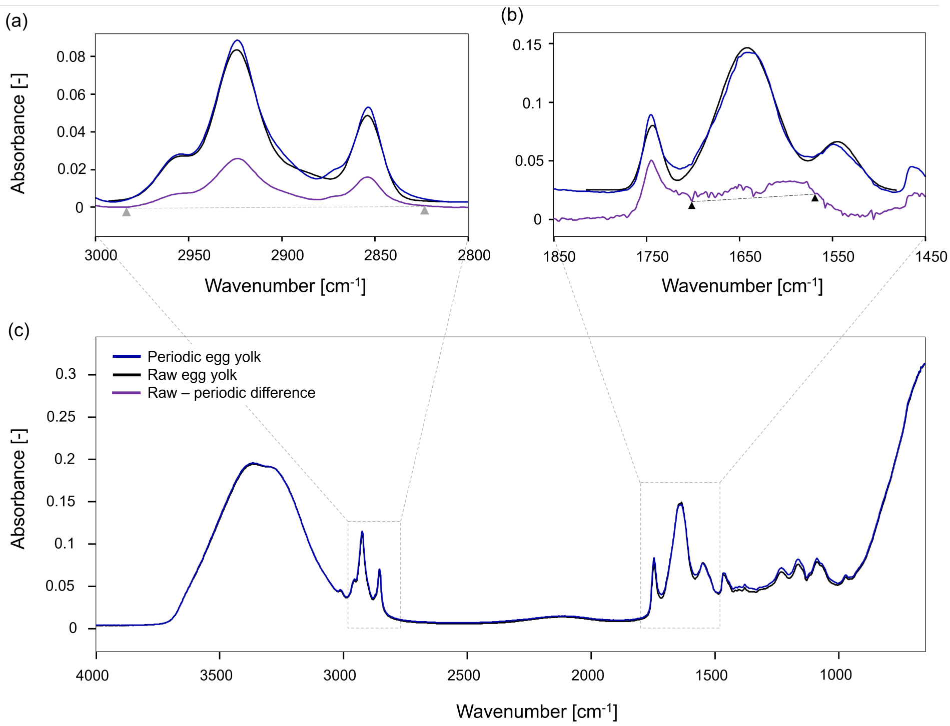

Fig. A6 IR spectra of raw and periodic egg yolk. IR spectra of raw (black) and periodic (blue) egg yolk over the whole IR range (c); close up on band no. 2 and 3 (a) and on band no. 4 and 5 (amide I region) (b) with addition of the difference spectrum magnified x5 (purple) and the baseline used for area quantification in the Amide I region (black dotted line) and in the region between 3000 and 2800 cm^{-1} (grey dotted line).

[10] Luz, C., Izzo, L., Graziani, G., Gaspari, A., Ritieni, A., Mañes, J., Meca, G.: Evaluation of biological and antimicrobial properties of freeze-dried whey fermented by different strains of lactobacillus plantarum. Food & function **9**(7), 3688–3697 (2018)

[11] Bermudez-Aguirre, D., Niemira, B.A.: A review on egg pasteurization and disinfection: Traditional and novel processing technologies. Comprehensive Reviews in Food Science and Food Safety **22**(2), 756–784 (2023)

[12] Stadelman, W., Singh, R., Muriana, P., Hou, H.: Pasteurization of eggs in the shell. Poultry Science **75**(9), 1122–1125 (1996)

[13] Licciardello, J.J., Nickerson, J., Goldblith, S.: Destruction of salmonellae in hard-boiled eggs. American Journal of Public Health and the Nations Health **55**(10), 1622–1628 (1965)

[14] Doyle, M.E., Mazzotta, A.S.: Review of studies on the thermal resistance of

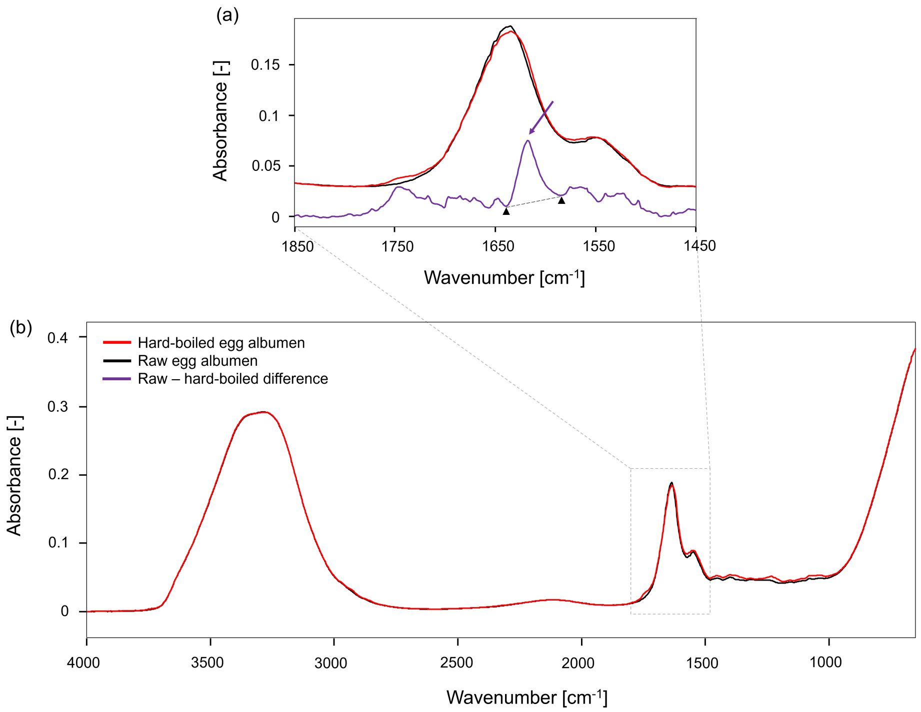

Fig. A7 IR spectra of raw and hard-boiled egg albumen. IR spectra of raw (black) and hard-boiled (red) egg albumen over the whole IR range (b); close up on band no. 4 and 5 (amide I region) (a) with addition of the difference spectrum magnified x5 (purple) and the baseline used for area quantification in the Amide I region (black dotted line). The purple arrow indicates the appearance of the aggregation band.

salmonellae. Journal of food protection **63**(6), 779–795 (2000)

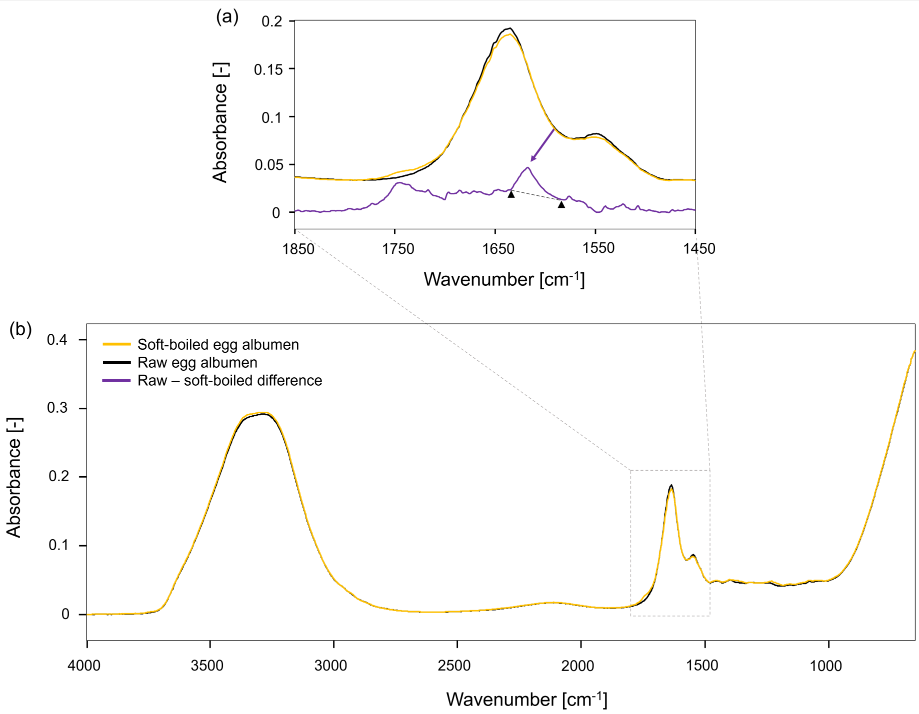

Fig. A8 IR spectra of raw and soft-boiled egg albumen. IR spectra of raw (black) and soft-boiled (orange) egg albumen over the whole IR range (b); close up on band no. 4 and 5 (amide I region) (a) with addition of the difference spectrum magnified x5 (purple) and the baseline used for area quantification in the Amide I region (black dotted line). The purple arrow indicates the appearance of the aggregation band.

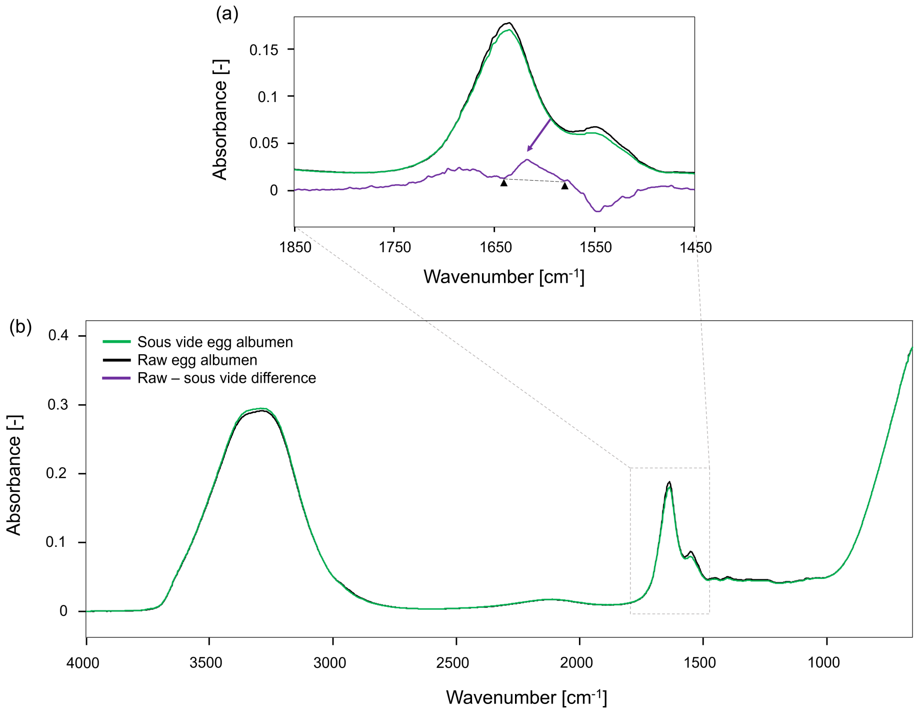

Fig. A9 IR spectra of raw and sous vide egg albumen. IR spectra of raw (black) and sous vide (green) egg albumen over the whole IR range (b); close up on band no. 4 and 5 (amide I region) (a) with addition of the difference spectrum magnified x5 (purple) and the baseline used for area quantification in the Amide I region (black dotted line). The purple arrow indicates the appearance of the aggregation band.

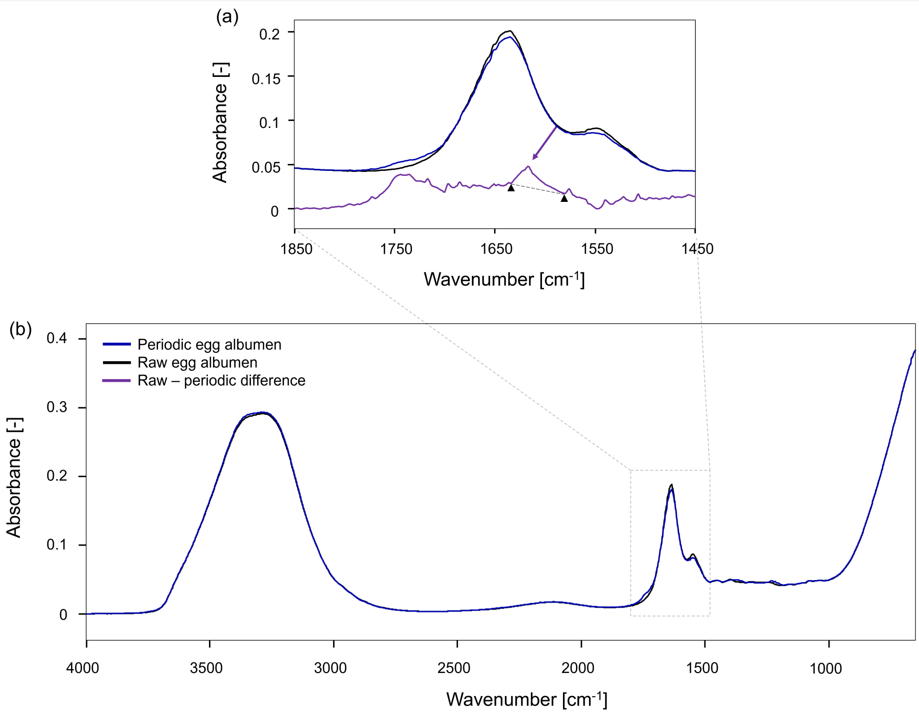

Fig. A10 IR spectra of raw and periodic egg albumen. IR spectra of raw (black) and periodic (blue) egg albumen over the whole IR range (b); close up on band no. 4 and 5 (amide I region) (a) with addition of the difference spectrum magnified x5 (purple) and the baseline used for area quantification in the Amide I region (black dotted line). The purple arrow indicates the appearance of the aggregation band.

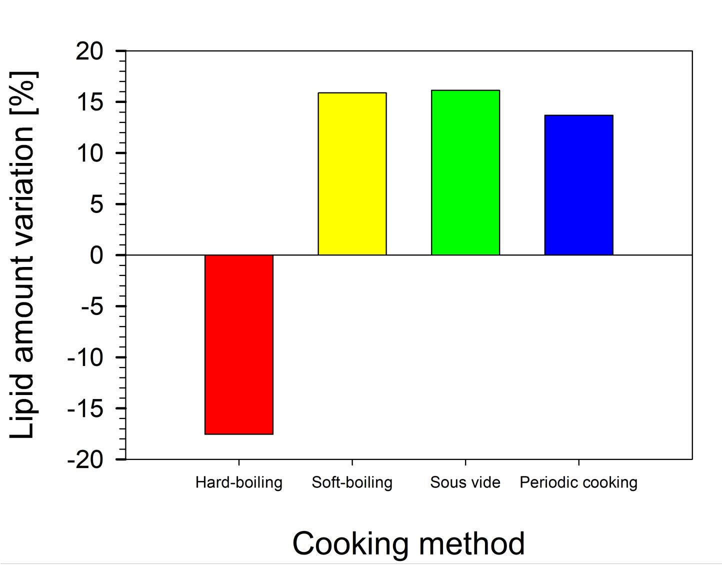

Fig. A11 Lipid amount variation during cooking. Lipid amount variation after cooking for four different cooking techniques: hard-boiling (red), soft-boiling (orange), 6X°C (green) and periodic cooking (blue).